

Supporting Information

Inter-Kramers Transitions and Spin-Phonon Couplings in a Lanthanide-Based Single-Molecule Magnet

Duncan H. Moseley,^a Shelby E. Stavretis,^a Zhenhua Zhu,^b Mei Guo,^b Craig M. Brown,^c Mykhaylo Ozerov,^d Yongqiang Cheng,^e Luke L. Daemen,^e Rachael Richardson,^f Gary Knight,^f Komalavalli Thirunavukkuarasu,^f Anibal J. Ramirez-Cuesta,^e Jinkui Tang,^b Zi-Ling Xue^{a,*}

^a Department of Chemistry, University of Tennessee, Knoxville, Tennessee 37996, United States

^b State Key Laboratory of Rare Earth Resource Utilization, Changchun Institute of Applied Chemistry, Chinese Academy of Sciences, Changchun 130022, P. R. China

^c Center for Neutron Research, National Institute of Standards and Technology, Gaithersburg, Maryland 20899, United States

^d National High Magnetic Field Laboratory, Tallahassee, Florida 32310, United States

^e Neutron Scattering Division, Oak Ridge National Laboratory, Oak Ridge, Tennessee 37831, United States

^f Department of Physics, Florida A&M University, Tallahassee, Florida 32307, United States

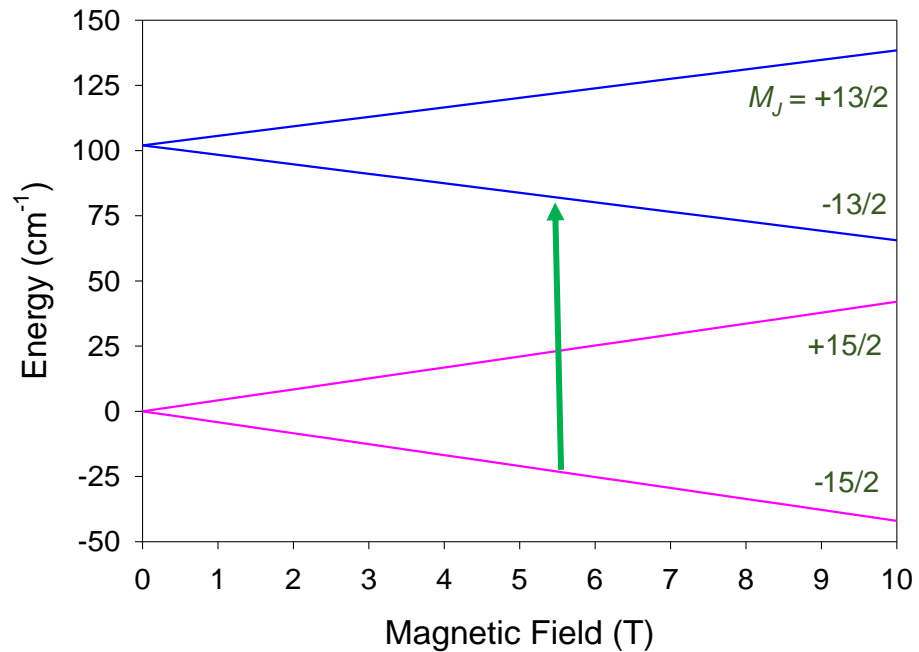


Figure S1. Zeeman splitting of the $M_J = \pm 13/2$ and $\pm 15/2$ levels inside magnetic field calculated with $g = 1.2$.^{S1} Green arrow represents the magnetic transition observed in far-IR and INS.

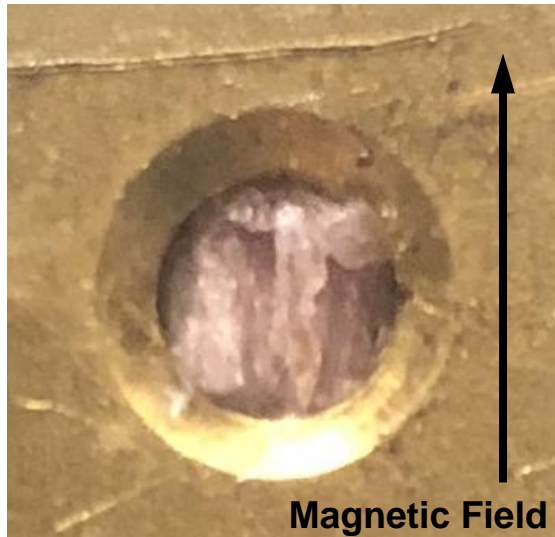


Figure S2. Image of the vertically-aligned crystal sample of **1**. The clear aperture of the sample holder is 3.175 mm (1/8 inch). Image was captured through the wall of a glove box, as the sample was still inside the glove box, leading to low-resolution of the image. Rough-looking texture is likely due to hardened eicosane coating on the crystals. Magnetic field direction is indicated by black arrow.

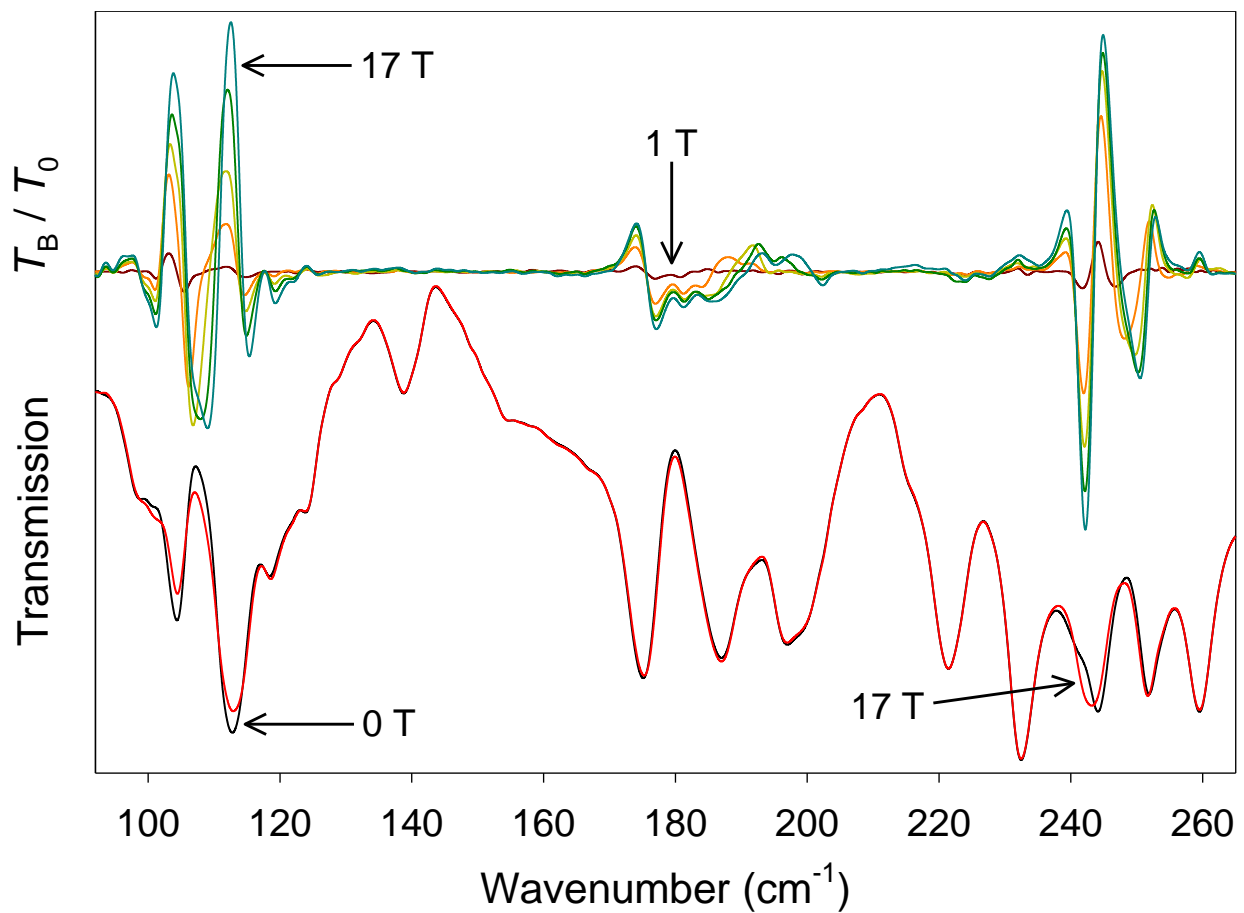


Figure S3. (Bottom) Far-IR transmission spectra of a powder sample of **1** at 0 (black) and 17 T (red); (Top) Transmission normalized to the zero-field spectrum T_B / T_0 at 1, 5 (orange), 9 (yellow green), 13 (green), and 17 T.

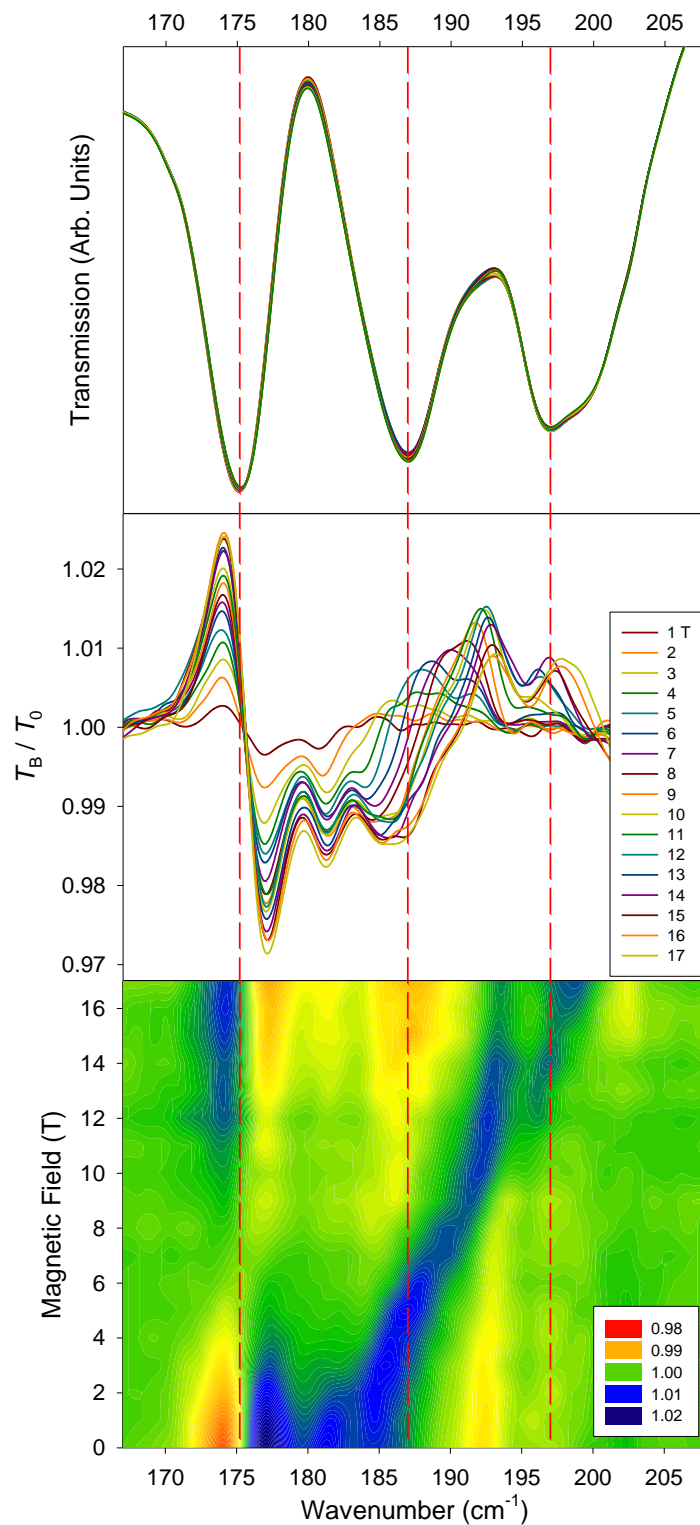


Figure S4. Far-IR spectra of the v_2 magnetic transition in a powder sample of **1**. (Top) Raw transmission; (Middle) Transmission normalized to the zero-field spectrum (T_0); (Bottom)

Contour plot of the normalized transmission (by average). Red lines indicate approximate zero-field position of major phonon peaks. *It is important to note that the blue portion indicates a lower intensity region compared to the average across all fields and is not a shifting peak.*

There are two intense phonons at 187 and 197 cm⁻¹ (Figure S4-Top), but they do not have clear couplings with the magnetic peak. One possible explanation for this behavior is that v₂ occurs at ~180 cm⁻¹ at 0 T, where it slightly repels the 176 cm⁻¹ peak to lower energies. As v₂ shifts to higher energies with applied fields, it appears to experience weak avoided crossings with phonons in the 185-200 cm⁻¹ range. Repeated studies with spectra from two different powder samples reveal a similar feature. The spectra of the crystal samples indicated a change in the same region, but was not as clear as the powder spectra.

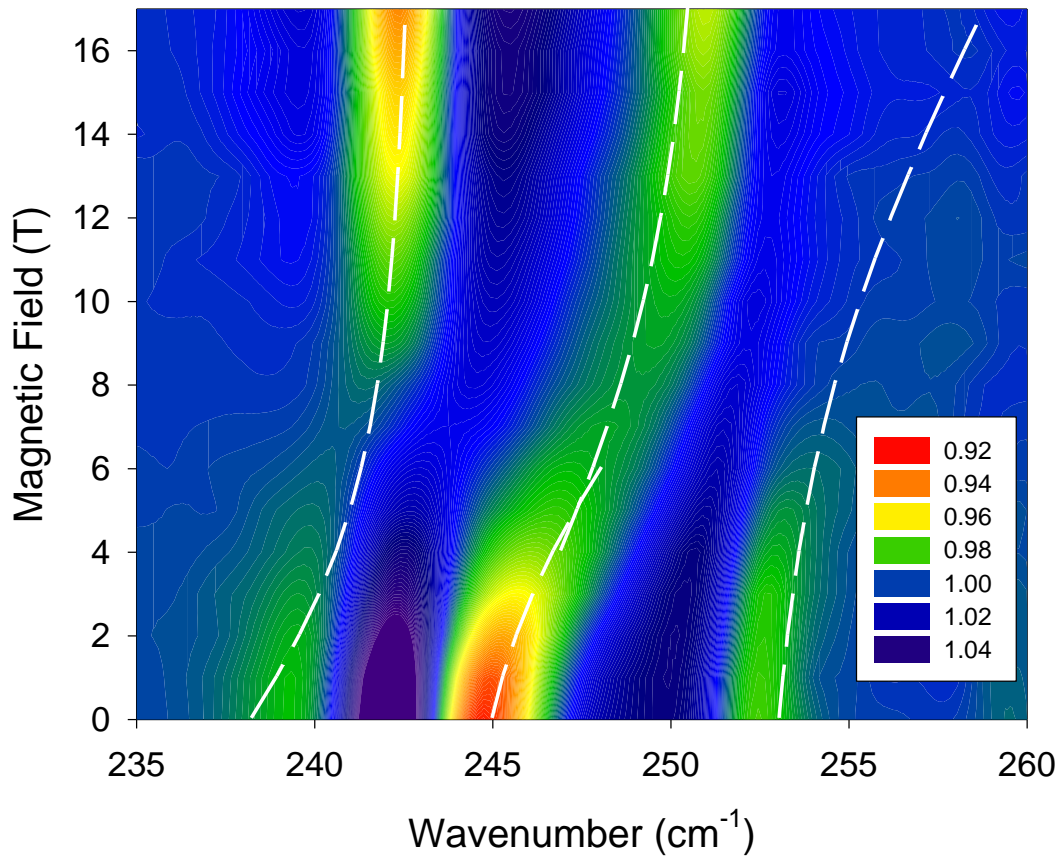


Figure S5. Contour plot showing the spin-phonon coupling model for v_3 in far-IR by two separate 2×2 matrix equations as in Eq. 1. Coupling constants Λ_1 and Λ_2 are $3.0(5)$ and $3.0(7) \text{ cm}^{-1}$, respectively.

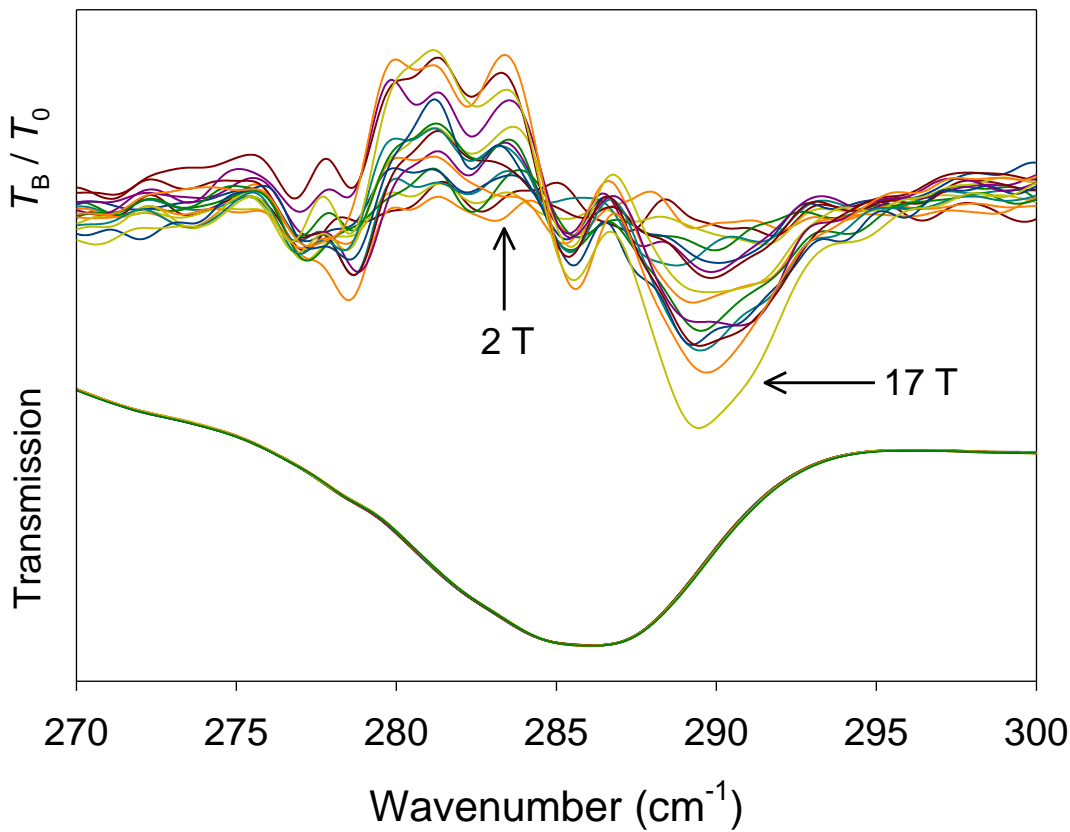


Figure S6. (Bottom) Far-IR transmission spectra of **1** at 0 (black) and 17 T (red); (Top) Transmission normalized to the zero-field spectrum T_B / T_0 , displaying a possible weak magnetic transition located at $\sim 285 \text{ cm}^{-1}$. This would theoretically correspond to the $-15/2 \rightarrow -7/2$ transition ν_4 , which also appears to shift to higher energies with field.

It is possible that the next transition (ν_4) can be viewed at approximately 285 cm^{-1} , as shown in Figure S3. However, this feature is very weak compared to ν_1 , ν_2 , and ν_3 , and does not appear to couple to any phonons in far-IR. However, this is not clear due to the weakness of the far-IR intensity.

Table S1. Fitting parameters of spin–phonon coupling in the crystal sample for Eqs. 1 and 5.^{a-c}

Since the magnetic peaks (v_i) were drawn as straight lines simulating linear shifts, the starting and ending energies at the initial (0 T) and final (17 T) fields are specified.

Peaks (E_{sp} and E_{ph}) ^a	v_1 - 0 T	v_1 - 17 T	Ph-1		Ph-2	v_3 - 0 T	v_3 - 17 T	Ph-3
Energy (cm⁻¹)^b	104.7(1.5)	115.5(5)	111.5(8)		243.0(5)	243(3)	267(6)	251.7(5)
A (cm⁻¹)^b	N/A	N/A	3.0(3)		3.0(5)	N/A	N/A	3.0(7)

^a Ph-1 refers to the phonon coupled to magnetic peak v_1 . Ph-2 and Ph-3 refer to the two phonons coupled to magnetic peak v_3 .

^b Errors are based on a visual inspection of the best fit of the contour plots, and are inherently difficult to estimate due to the multi-parameter nature of the fitting. For example, altering the phonon energies can slightly change the coupling constants and slope of v_i required for a good fit. Thus, all errors stem from the alteration of a single parameter at a time.

^c The energies in the table, such as v_1 and Ph-1 as well as v_3 , Ph-2 and Ph-3, are the best-fit values. They may deviate from the observed values from the spectra in Figure 3-Bottom.

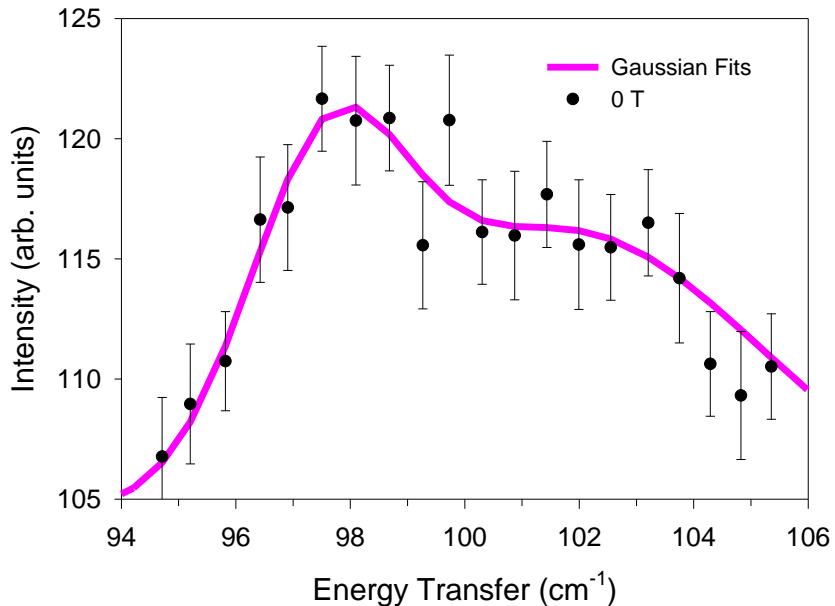


Figure S7. Fitting of the phonon and magnetic peaks in $\text{Er}[\text{N}(\text{SiMe}_3)_2]_3$ (**1**) with Gaussian functions at 0 T.

Table S2. Area and FWHM (full width at half maximum) of the phonon peak located at 115 cm^{-1} at 10 T. At this field, the magnetic peak is a shoulder off this phonon.

	Area	FWHM (cm^{-1})
0 T	53.9	7.20
10 T	55.7	8.56
% Difference	3.2%	15.9%

Deconvolutions of the overlapping peaks involving the magnetic transition in INS spectra at DCS at 0 T (1.7 K, Figure 5) and at VISION at 5 K (Figure 6) give the magnetic peak at 104.0 cm^{-1} (FWHM = 3.2 cm^{-1}) and 103.6 cm^{-1} (FWHM = 3.5 cm^{-1}), respectively. Thus, 104 cm^{-1} was chosen as the magnetic transition with $\approx 1 \text{ cm}^{-1}$ as the error.

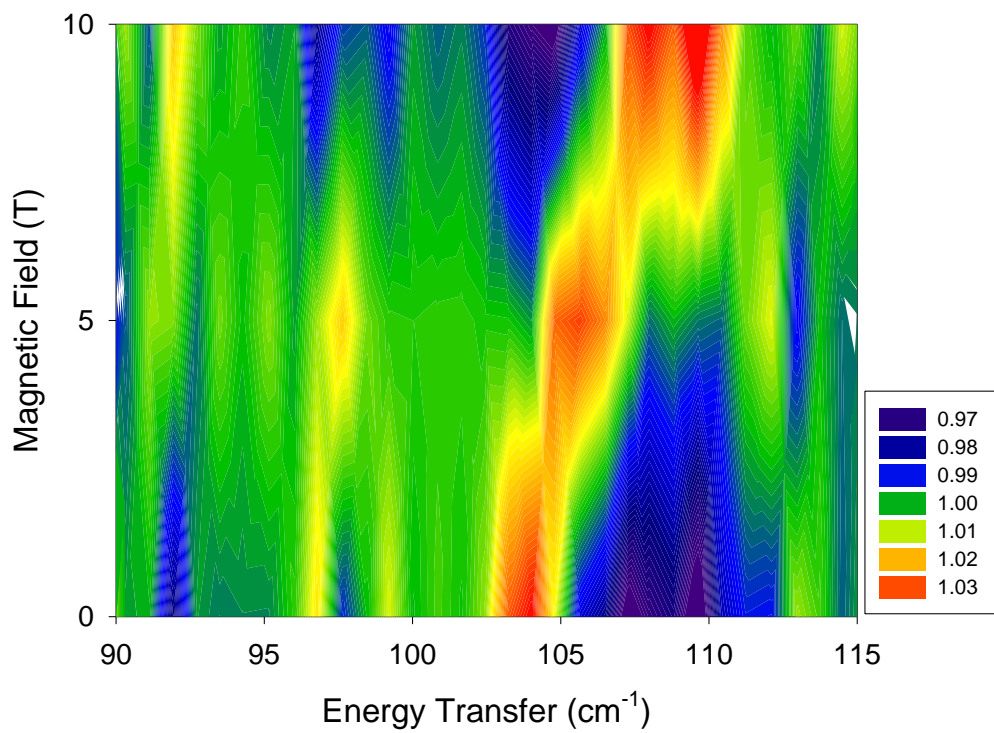
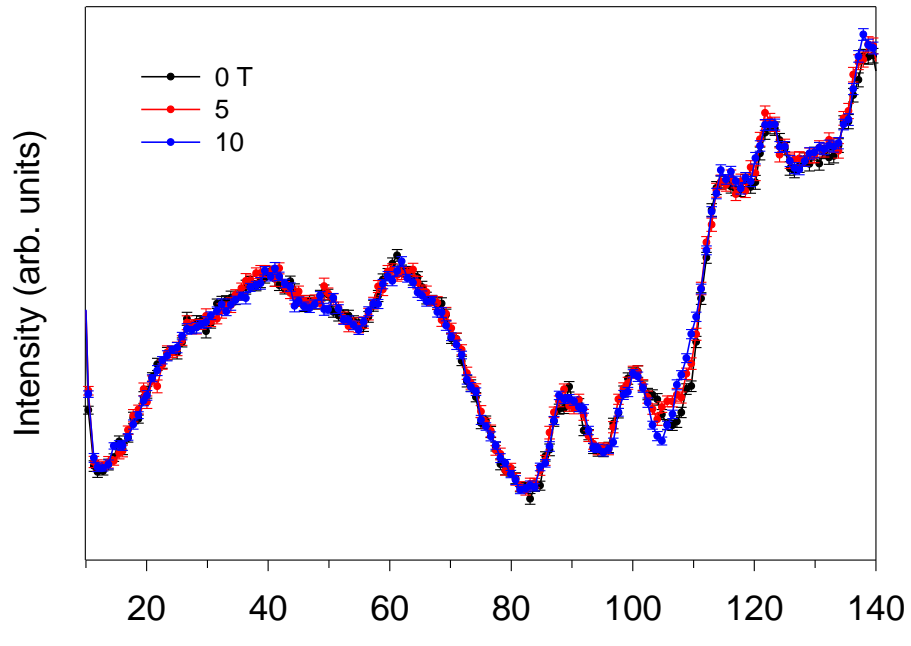


Figure S8. (Top) Complete INS spectra (DCS) at 1.5 K at 0 (black), 5 (red), and 10 T (blue) with $E_i = 201.6 \text{ cm}^{-1}$. (Bottom) Contour plot of the normalized scattering intensity (by average).

It is noted that very limited INS data, at just 0, 5 and 10 T, are available for the contour plot.

Raman Measurements under Magnetic Fields

Raman spectroscopy is a very widely used method to probe the inter-Kramers-doublet transitions of lanthanide ions in solids,^{S2-3} including lanthanide halides and hydroxides, lanthanide-doped garnet crystals (e.g., Nd³⁺:Y₃Al₅O₁₂ or the Nd:YAG laser material) or other host lattices,^{S3} and lanthanide aluminates (e.g., NdAlO₃).^{S3} The inter-Kramers-doublet are Raman-active if they follow the electronic Raman selection rules of $\Delta J \leq 2$, $\Delta L \leq 2$, $\Delta S = 0$. However, electronic Raman selection rules tend to be less strict than their vibrational counterparts.^{S3-4} Analyses by the selection rules indicate that the transitions, $M_J = \pm 15/2 \rightarrow \pm 13/2$, $M_J = \pm 15/2 \rightarrow \pm 11/2$ and $M_J = \pm 15/2 \rightarrow \pm 9/2$, should be allowed in Raman spectroscopy.^{S3-5}

We attempted field-dependent Raman using a direct optics setup coupled with a 14 T magnet. The sample was mounted inside an air-sensitive sample stage using an argon glove box, where the outer layer of the crystal was sheared off. Data were collected by a backscattering Faraday geometry using a 532 nm free-beam laser at 5 K in a 14 T SCM in the Electron Magnetic Resonance (EMR) facility. Collected scattered light was guided to a spectrometer equipped with a liquid-nitrogen-cooled CCD camera. It should be pointed out that, despite the precautions including the use of the air-sensitive sample stage, it is possible that the crystal still experienced some slight decomposition.

Our Raman spectra (Figure S6) showed two field-dependent features at approximately 290 cm⁻¹ (which was coupled to a nearby phonon) and 556 cm⁻¹ (which displayed as an inverted peak that split under field). The first is relatively close to the supposed v₄ transition. However, we were unable to explain the behavior of the latter and reliably assign it to any transition. These data had an abnormally large background, which could be due to either the extreme moisture-

sensitivity of the sample leading to degradation or fluorescence due to the 532 nm laser. We may reattempt the sample in the future using a different laser wavelength to combat possible fluorescence.

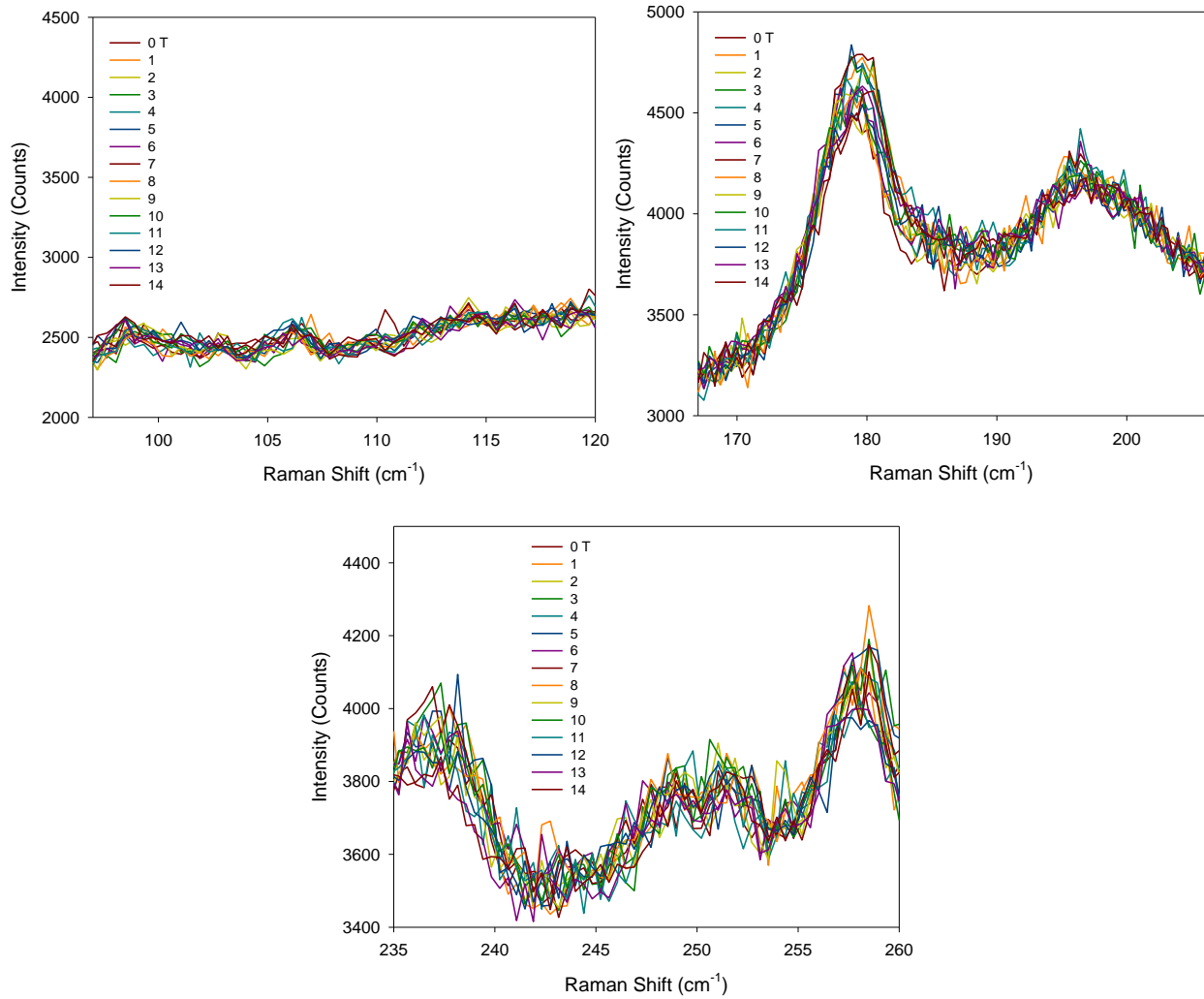


Figure S9. Raman spectra under magnetic fields: (Top-Left) 97-120 cm⁻¹; (Top-Right) 167-206 cm⁻¹; (Bottom) 235-260 cm⁻¹. These regions correspond to the regions in far-IR in Figures 3, 4 and S4.

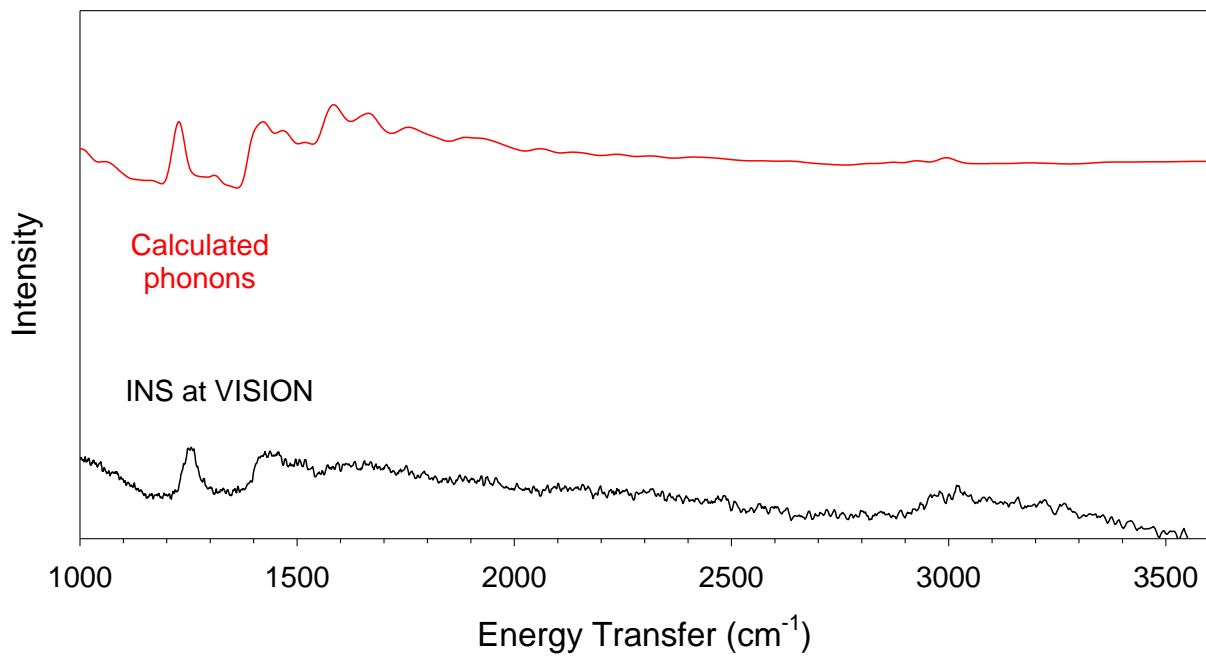


Figure S10. INS spectrum (VISION) at 5 K in the $1000\text{-}3600\text{ cm}^{-1}$ range in comparison with the calculated phonons.

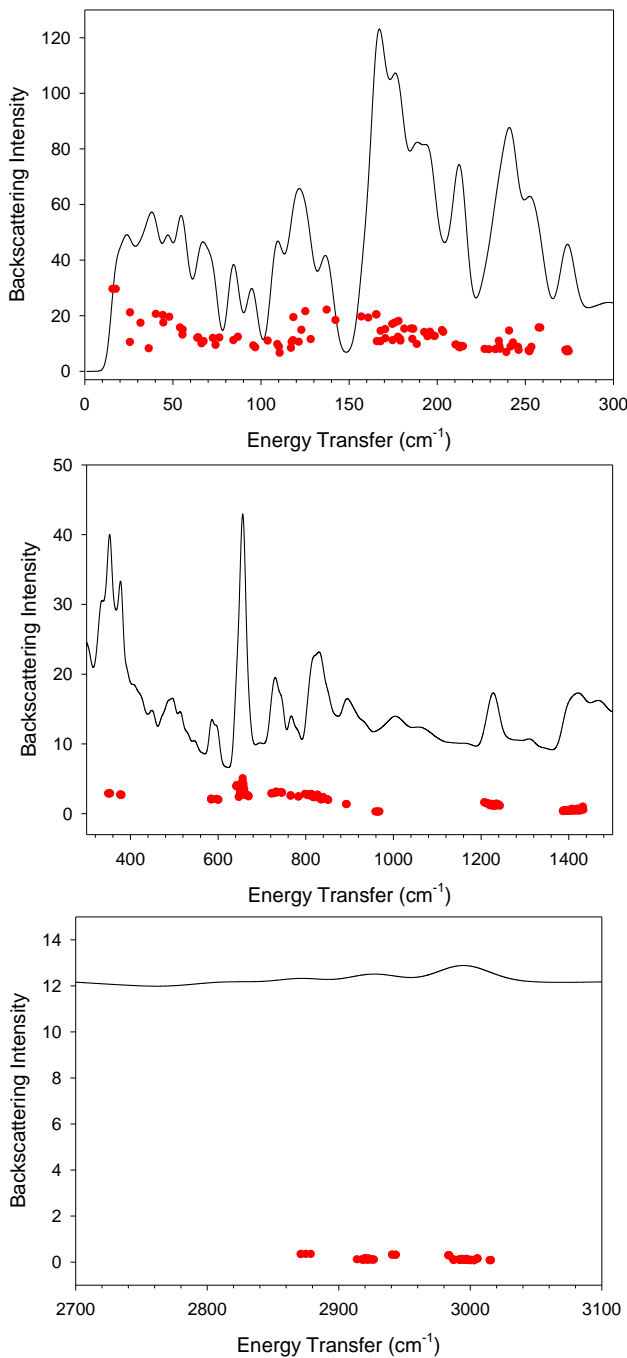


Figure S11. Calculated backscattering INS spectrum (black line) and peak intensities (red points) in the 0-300 cm⁻¹ (Top), 300-1500 cm⁻¹ (Middle) and 2700-3100 cm⁻¹ (Bottom) regions. Other regions contained no calculated peaks. Note that while the spectrum is calculate for the entire Brillouin zone, the peak intensities are only calculated for the gamma point.^{S6}

Table S3. Calculated Phonons in Er[N(SiMe₃)₂]₃ (**1**) and Their Intensities^{a,b}

Phonon No.	Energy (cm⁻¹)	Symmetry	Back^c	Forward^c
[4]	15.85	<i>A_u</i>	29.57	6.79
[5, 6]	17.73	<i>E_{g/u}</i>	29.56	6.93
[7]	25.77	<i>A_g</i>	10.44	2.56
[8, 9]	25.81	<i>E_{g/u}</i>	21.09	5.28
[10]	31.74	<i>A_g</i>	17.35	4.65
[11, 12]	36.44	<i>E_{g/u}</i>	8.17	2.21
[13, 14]	40.47	<i>E_{g/u}</i>	20.54	6.01
[15]	44.41	<i>A_u</i>	20.14	6.08
[16]	44.72	<i>A_g</i>	17.44	5.21
[17, 18]	48.10	<i>E_{g/u}</i>	19.50	6.13
[19, 20]	54.22	<i>E_{g/u}</i>	15.62	5.03
[21]	55.58	<i>A_u</i>	13.10	4.24
[22, 23]	55.70	<i>E_{g/u}</i>	14.89	4.81
[24]	63.96	<i>A_g</i>	11.95	4.03
[25, 26]	64.52	<i>E_{g/u}</i>	12.12	4.20
[27]	66.36	<i>A_g</i>	9.95	3.48
[28]	67.59	<i>A_u</i>	10.74	3.84
[29]	72.84	<i>A_g</i>	11.87	4.29
[30, 31]	74.36	<i>E_{g/u}</i>	9.40	3.48
[32]	76.46	<i>A_u</i>	12.02	4.43
[33, 34]	84.46	<i>E_{g/u}</i>	11.09	4.28
[35, 36]	87.05	<i>E_{g/u}</i>	12.29	4.89
[37, 38]	95.80	<i>E_{g/u}</i>	9.16	3.75
[39, 40]	96.89	<i>E_{g/u}</i>	8.52	3.49
[41]	103.92	<i>A_u</i>	10.91	4.89
[42, 43]	109.38	<i>E_{g/u}</i>	9.67	4.44
[44, 45]	110.30	<i>E_{g/u}</i>	8.77	4.04
[46]	110.74	<i>A_g</i>	6.56	2.97
[47]	117.15	<i>A_u</i>	8.35	4.02

Phonon No.	Energy (cm⁻¹)	Symmetry	Back^c	Forward^c
[48]	117.54	A_g	10.51	5.05
[49]	118.27	A_u	11.09	5.41
[50, 51]	118.51	$E_{g/u}$	19.38	9.81
[52, 53]	121.51	$E_{g/u}$	10.51	5.13
[54, 55]	123.04	$E_{g/u}$	14.81	7.64
[56]	125.30	A_g	21.51	11.47
[57]	128.37	A_g	11.45	5.85
[58, 59]	137.46	$E_{g/u}$	22.08	12.42
[60]	142.39	A_u	18.32	10.52
[61]	157.03	A_u	19.58	11.75
[62]	161.00	A_g	19.21	11.62
[63, 64]	165.43	$E_{g/u}$	20.36	12.45
[65, 66]	165.71	$E_{g/u}$	20.36	12.29
[67]	165.85	A_g	10.72	6.35
[68]	167.99	A_u	10.71	6.37
[69, 70]	168.01	$E_{g/u}$	14.45	8.81
[71, 72]	170.59	$E_{g/u}$	15.04	9.36
[73, 74]	170.79	$E_{g/u}$	11.79	7.18
[75, 76]	174.62	$E_{g/u}$	16.92	10.81
[77]	174.83	A_g	11.10	6.67
[78]	175.97	A_u	17.37	10.92
[79, 80]	177.84	$E_{g/u}$	12.28	7.70
[81]	178.19	A_g	18.00	11.51
[82, 83]	179.00	$E_{g/u}$	11.60	7.26
[84]	179.32	A_u	10.92	6.74
[85]	181.48	A_g	15.21	9.94
[86, 87]	185.29	$E_{g/u}$	15.31	10.11
[88, 89]	186.01	$E_{g/u}$	11.54	7.42
[90]	186.58	A_u	15.19	10.10
[91, 92]	188.55	$E_{g/u}$	9.70	6.07
[93, 94]	192.79	$E_{g/u}$	13.99	9.34

Phonon No.	Energy (cm⁻¹)	Symmetry	Back^c	Forward^c
[95]	194.58	A_u	12.50	8.39
[96, 97]	196.03	$E_{g/u}$	14.10	9.86
[98, 99]	197.89	$E_{g/u}$	12.75	8.98
[100]	198.77	A_g	12.59	8.70
[101]	202.83	A_u	14.67	10.30
[102]	203.57	A_g	14.09	9.85
[103, 104]	210.50	$E_{g/u}$	9.51	6.33
[105, 106]	211.13	$E_{g/u}$	9.45	6.21
[107]	212.59	A_g	8.57	5.61
[108]	213.02	A_u	8.50	5.52
[109, 110]	213.73	$E_{g/u}$	9.00	5.77
[111, 112]	214.79	$E_{g/u}$	8.92	5.80
[113]	227.02	A_u	7.92	5.41
[114]	229.46	A_g	7.81	5.34
[115, 116]	233.14	$E_{g/u}$	7.83	5.31
[117, 118]	235.10	$E_{g/u}$	10.85	7.31
[119]	235.42	A_g	9.04	6.15
[120]	235.69	A_u	7.97	5.42
[121]	239.34	A_g	6.83	4.72
[122, 123]	240.95	$E_{g/u}$	14.55	9.95
[124, 125]	241.77	$E_{g/u}$	8.78	6.05
[126, 127]	243.12	$E_{g/u}$	10.25	7.24
[128, 129]	245.97	$E_{g/u}$	8.64	6.08
[130]	246.31	A_u	7.57	5.27
[131]	252.02	A_g	7.47	5.58
[132]	252.43	A_u	7.08	5.280
[133, 134]	252.58	$E_{g/u}$	7.37	5.33
[135, 136]	253.56	$E_{g/u}$	8.69	6.25
[137]	257.70	A_u	15.63	11.11
[138]	258.64	A_g	15.61	11.16
[139]	272.88	A_g	7.60	5.29

Phonon No.	Energy (cm⁻¹)	Symmetry	Back^c	Forward^c
[140, 141]	273.62	$E_{g/u}$	7.03	5.05
[142]	274.17	A_u	7.80	5.49
[143, 144]	274.74	$E_{g/u}$	7.11	5.11
[145]	349.87	A_u	2.85	2.40
[146]	352.13	A_g	2.85	2.42
[147, 148]	353.50	$E_{g/u}$	2.83	2.40
[149, 150]	354.11	$E_{g/u}$	2.86	2.43
[151]	377.11	A_u	2.68	2.37
[152, 153]	378.84	$E_{g/u}$	2.65	2.34
[154]	378.94	A_g	2.69	2.38
[155, 156]	380.21	$E_{g/u}$	2.64	2.33
[157]	584.84	A_u	2.09	2.19
[158]	585.06	A_g	2.05	2.15
[159, 160]	585.13	$E_{g/u}$	2.01	2.12
[161, 162]	585.38	$E_{g/u}$	2.00	2.12
[163, 164]	597.05	$E_{g/u}$	2.05	2.25
[165, 166]	597.23	$E_{g/u}$	2.04	2.24
[167]	601.01	A_u	1.97	2.20
[168]	601.04	A_g	1.96	2.19
[169, 170]	642.66	$E_{g/u}$	3.90	4.52
[171]	642.66	A_u	3.89	4.52
[172, 173]	642.78	$E_{g/u}$	3.90	4.53
[174]	643.17	A_g	4.05	4.72
[175, 176]	647.99	$E_{g/u}$	2.41	2.85
[177, 178]	648.13	$E_{g/u}$	2.35	2.76
[179]	650.79	A_u	3.16	3.76
[180]	651.01	A_g	3.12	3.75
[181]	654.32	A_g	4.36	5.52
[182, 183]	654.8	$E_{g/u}$	3.15	4.07
[184, 185]	654.87	$E_{g/u}$	3.53	4.42
[186]	654.91	A_u	3.29	4.33

Phonon No.	Energy (cm⁻¹)	Symmetry	Back^c	Forward^c
[187, 188]	655.98	$E_{g/u}$	4.51	5.76
[189]	656.58	A_g	3.72	4.64
[190, 191]	656.68	$E_{g/u}$	4.59	5.61
[192]	656.74	A_u	5.03	6.22
[193, 194]	658.04	$E_{g/u}$	4.12	5.17
[195, 196]	658.14	$E_{g/u}$	4.27	5.43
[197]	658.26	A_g	3.96	5.00
[198]	660.19	A_u	3.52	4.45
[199, 200]	661.38	$E_{g/u}$	2.67	3.42
[201]	661.39	A_g	2.62	3.37
[202, 203]	662.02	$E_{g/u}$	2.84	3.70
[204]	662.58	A_u	2.86	3.57
[205]	668.33	A_u	2.55	3.16
[206, 207]	669.53	$E_{g/u}$	2.55	3.14
[208]	669.62	A_g	2.45	3.03
[209, 210]	670.56	$E_{g/u}$	2.47	3.06
[211, 212]	722.42	$E_{g/u}$	2.84	3.68
[213, 214]	722.77	$E_{g/u}$	2.89	3.75
[215]	726.64	A_u	2.91	3.89
[216]	727.18	A_g	2.88	3.83
[217]	733.06	A_g	3.09	4.24
[218, 219]	733.52	$E_{g/u}$	3.02	4.14
[220, 221]	733.56	$E_{g/u}$	2.97	4.07
[222]	733.58	A_u	3.08	4.22
[223]	743.28	A_g	3.02	4.13
[224, 225]	744.06	$E_{g/u}$	3.04	4.18
[226]	746.16	A_u	2.96	4.05
[227, 228]	746.19	$E_{g/u}$	3.00	4.14
[229, 230]	765.98	$E_{g/u}$	2.52	3.41
[231, 232]	766.32	$E_{g/u}$	2.60	3.53
[233]	783.37	A_g	2.40	3.37

Phonon No.	Energy (cm⁻¹)	Symmetry	Back^c	Forward^c
[234]	784.52	A_u	2.42	3.39
[235]	798.95	A_g	2.78	3.99
[236]	803.75	A_u	2.63	3.81
[237, 238]	804.69	$E_{g/u}$	2.75	3.95
[239, 240]	807.00	$E_{g/u}$	2.60	3.79
[241, 242]	813.14	$E_{g/u}$	2.78	3.84
[243]	813.21	A_u	2.50	3.70
[244, 245]	814.35	$E_{g/u}$	2.71	3.78
[246, 247]	816.14	$E_{g/u}$	2.45	3.66
[248, 249]	818.34	$E_{g/u}$	2.30	3.49
[250]	819.17	A_g	2.33	3.53
[251, 252]	825.86	$E_{g/u}$	2.32	3.40
[253, 254]	826.59	$E_{g/u}$	2.38	3.44
[255]	826.70	A_u	2.58	3.62
[256]	827.62	A_g	2.69	3.72
[257]	832.81	A_g	2.19	3.29
[258, 259]	835.42	$E_{g/u}$	1.99	3.01
[260]	836.27	A_u	2.09	3.16
[261, 262]	839.63	$E_{g/u}$	2.04	3.07
[263]	840.56	A_u	2.34	3.45
[264]	841.06	A_g	2.23	3.31
[265, 266]	850.20	$E_{g/u}$	2.01	3.01
[267, 268]	851.99	$E_{g/u}$	1.92	2.87
[269]	892.52	A_u	1.33	2.00
[270]	894.19	A_g	1.32	1.98
[271, 272]	959.65	$E_{g/u}$	0.26	0.21
[273]	964.32	A_u	0.25	0.20
[274]	964.58	A_g	0.25	0.20
[275, 276]	968.77	$E_{g/u}$	0.26	0.22
[277]	1208.07	A_u	1.56	2.82
[278]	1208.42	A_g	1.58	2.84

Phonon No.	Energy (cm⁻¹)	Symmetry	Back^c	Forward^c
[279, 280]	1212.54	$E_{g/u}$	1.42	2.65
[281, 282]	1214.07	$E_{g/u}$	1.49	2.73
[283]	1220.19	A_u	1.17	2.33
[284]	1220.77	A_g	1.30	2.49
[285, 286]	1221.08	$E_{g/u}$	1.23	2.40
[287]	1222.37	A_u	1.37	2.57
[288, 289]	1222.93	$E_{g/u}$	1.21	2.38
[290]	1223.21	A_g	1.18	2.33
[291, 292]	1223.67	$E_{g/u}$	1.13	2.27
[293, 294]	1224.53	$E_{g/u}$	1.26	2.43
[295]	1227.64	A_u	1.25	2.42
[296, 297]	1228.15	$E_{g/u}$	1.17	2.32
[298]	1228.45	A_g	1.28	2.47
[299, 300]	1228.57	$E_{g/u}$	1.11	2.25
[301]	1230.18	A_u	1.10	2.23
[302]	1231.29	A_g	1.11	2.26
[303]	1234.95	A_g	1.11	2.25
[304, 305]	1235.32	$E_{g/u}$	1.18	2.33
[306, 307]	1235.56	$E_{g/u}$	1.40	2.61
[308, 309]	1240.66	$E_{g/u}$	1.17	2.34
[310, 311]	1240.81	$E_{g/u}$	1.28	2.47
[312]	1243.56	A_u	1.09	2.24
[313]	1387.24	A_g	0.36	1.09
[314, 315]	1387.63	$E_{g/u}$	0.31	0.98
[316, 317]	1389.39	$E_{g/u}$	0.41	1.18
[318, 319]	1389.83	$E_{g/u}$	0.39	1.15
[320]	1390.65	A_g	0.37	1.11
[321]	1391.27	A_u	0.41	1.19
[322]	1391.64	A_g	0.40	1.16
[323, 324]	1391.94	$E_{g/u}$	0.44	1.23
[325, 326]	1392.23	$E_{g/u}$	0.36	1.08

Phonon No.	Energy (cm⁻¹)	Symmetry	Back^c	Forward^c
[327]	1394.11	A_u	0.38	1.14
[328, 329]	1394.57	$E_{g/u}$	0.39	1.16
[330]	1394.79	A_u	0.42	1.21
[331, 332]	1395.41	$E_{g/u}$	0.39	1.15
[333, 334]	1397.05	$E_{g/u}$	0.43	1.22
[335]	1397.21	A_u	0.37	1.11
[336]	1398.50	A_g	0.43	1.23
[337, 338]	1399.59	$E_{g/u}$	0.44	1.25
[339]	1399.69	A_g	0.35	1.07
[340]	1399.79	A_u	0.41	1.15
[341, 342]	1399.96	$E_{g/u}$	0.49	1.32
[343, 344]	1402.88	$E_{g/u}$	0.44	1.22
[345]	1403.56	A_g	0.39	1.15
[346]	1403.92	A_u	0.39	1.13
[347, 348]	1403.92	$E_{g/u}$	0.49	1.30
[349]	1405.69	A_u	0.47	1.27
[350, 351]	1408.08	$E_{g/u}$	0.64	1.55
[352]	1408.24	A_g	0.53	1.36
[353, 354]	1408.87	$E_{g/u}$	0.44	1.22
[355, 356]	1411.04	$E_{g/u}$	0.40	1.15
[357, 358]	1411.54	$E_{g/u}$	0.51	1.36
[359]	1411.73	A_g	0.46	1.26
[360]	1412.84	A_u	0.45	1.23
[361, 362]	1414.49	$E_{g/u}$	0.43	1.19
[363, 364]	1417.19	$E_{g/u}$	0.54	1.38
[365]	1417.98	A_u	0.51	1.31
[366]	1418.16	A_g	0.61	1.52
[367, 368]	1418.57	$E_{g/u}$	0.40	1.15
[369, 370]	1419.45	$E_{g/u}$	0.45	1.25
[371]	1420.29	A_g	0.65	1.56
[372]	1422.80	A_u	0.55	1.41

Phonon No.	Energy (cm⁻¹)	Symmetry	Back^c	Forward^c
[373]	1425.56	A_u	0.63	1.53
[374, 375]	1425.59	$E_{g/u}$	0.36	1.06
[376, 377]	1426.80	$E_{g/u}$	0.58	1.44
[378]	1427.61	A_g	0.70	1.62
[379]	1430.21	A_u	0.79	1.80
[380, 381]	1432.57	$E_{g/u}$	0.96	2.06
[382, 383]	1433.21	$E_{g/u}$	0.87	1.91
[384]	1434.15	A_g	0.52	1.33
[385, 386]	2871.25	$E_{g/u}$	0.34	0.80
[387, 388]	2871.54	$E_{g/u}$	0.34	0.80
[389]	2875.22	A_g	0.34	0.81
[390]	2879.03	A_u	0.34	0.80
[391]	2914.01	A_g	0.11	0.33
[392]	2918.05	A_g	0.10	0.33
[393, 394]	2918.25	$E_{g/u}$	0.09	0.30
[395, 396]	2918.44	$E_{g/u}$	0.10	0.31
[397]	2919.13	A_u	0.10	0.31
[398, 399]	2919.88	$E_{g/u}$	0.15	0.44
[400]	2919.98	A_g	0.10	0.32
[401, 402]	2920.81	$E_{g/u}$	0.14	0.42
[403]	2921.04	A_g	0.14	0.42
[404, 405]	2921.06	$E_{g/u}$	0.11	0.34
[406]	2921.59	A_u	0.11	0.35
[407, 408]	2921.86	$E_{g/u}$	0.11	0.35
[409, 410]	2921.90	$E_{g/u}$	0.10	0.32
[411]	2922.69	A_u	0.10	0.32
[412, 413]	2923.06	$E_{g/u}$	0.10	0.32
[414]	2923.26	A_u	0.14	0.42
[415]	2924.27	A_g	0.10	0.32
[416, 417]	2925.52	$E_{g/u}$	0.10	0.31
[418]	2926.38	A_u	0.10	0.31

Phonon No.	Energy (cm⁻¹)	Symmetry	Back^c	Forward^c
[419, 420]	2926.97	$E_{g/u}$	0.10	0.31
[421, 422]	2940.81	$E_{g/u}$	0.31	0.73
[423, 424]	2940.84	$E_{g/u}$	0.31	0.73
[425]	2943.40	A_g	0.30	0.72
[426]	2943.69	A_u	0.30	0.72
[427]	2983.50	A_g	0.28	0.68
[428, 429]	2983.79	$E_{g/u}$	0.28	0.68
[430, 431]	2983.93	$E_{g/u}$	0.28	0.68
[432]	2984.35	A_u	0.28	0.68
[433]	2987.41	A_g	0.10	0.28
[434]	2987.55	A_u	0.09	0.28
[435, 436]	2987.56	$E_{g/u}$	0.09	0.29
[437, 438]	2987.76	$E_{g/u}$	0.09	0.29
[439]	2991.60	A_u	0.09	0.29
[440, 441]	2991.62	$E_{g/u}$	0.10	0.30
[442, 443]	2992.73	$E_{g/u}$	0.09	0.29
[444]	2992.78	A_g	0.09	0.29
[445]	2993.58	A_g	0.09	0.29
[446, 447]	2993.83	$E_{g/u}$	0.12	0.35
[448, 449]	2993.85	$E_{g/u}$	0.12	0.36
[450, 451]	2994.49	$E_{g/u}$	0.11	0.31
[452]	2994.92	A_u	0.09	0.28
[453, 454]	2995.35	$E_{g/u}$	0.10	0.30
[455]	2996.47	A_g	0.09	0.28
[456]	2997.05	A_u	0.11	0.35
[457]	2997.37	A_g	0.12	0.36
[458, 459]	2997.48	$E_{g/u}$	0.09	0.27
[460, 461]	2998.21	$E_{g/u}$	0.08	0.26
[462]	2998.27	A_g	0.08	0.25
[463]	2998.43	A_u	0.08	0.26
[464, 465]	2998.54	$E_{g/u}$	0.08	0.26

Phonon No.	Energy (cm⁻¹)	Symmetry	Back	Forward^c
[466, 467]	2998.56	$E_{g/u}$	0.07	0.24
[468]	2998.92	A_u	0.09	0.29
[469]	3000.83	A_g	0.08	0.25
[470, 471]	3001.00	$E_{g/u}$	0.07	0.25
[472, 473]	3001.04	$E_{g/u}$	0.07	0.25
[474]	3001.43	A_u	0.07	0.25
[475]	3002.81	A_u	0.07	0.24
[476]	3003.02	A_g	0.07	0.25
[477, 478]	3003.12	$E_{g/u}$	0.07	0.24
[479, 480]	3003.17	$E_{g/u}$	0.07	0.24
[481]	3005.27	A_g	0.14	0.40
[482]	3005.47	A_u	0.14	0.39
[483, 484]	3005.62	$E_{g/u}$	0.14	0.39
[485, 486]	3005.88	$E_{g/u}$	0.14	0.40
[487]	3014.97	A_g	0.07	0.24
[488, 489]	3015.18	$E_{g/u}$	0.07	0.24
[490]	3015.85	A_u	0.07	0.24
[491, 492]	3015.88	$E_{g/u}$	0.07	0.24

^a The crystal structure of **1** (trigonal, space group $P-31c$, number 163) has D_{3d} symmetry. The symmetries of the phonon modes are thus in D_{3d} .

^b Phonopy is not currently able to assign the doubly-degenerated E vibrations. Thus, the calculated E phonons are labeled as both g and u .

^c “Back” and “Forward” refer to the calculated back- and forward-scattering INS intensities.

References for SI

- S1. Köbler, U.; Hoser, A., *Renormalization Group Theory. Impact on Experimental Magnetism*. Springer-Verlag Berlin Heidelberg: 2010.
- S2. Koningstein, J. A.; Grunberg, P., Electronic Raman Spectra. VII. Raman Spectra of the Lanthanides. *Can. J. Chem.* **1971**, *49*, 2336-2344.
- S3. Clark, R. J. H.; Dines, T. J., Electronic Raman spectroscopy. In *Advances in Infrared and Raman Spectroscopy*, Vol. 9, Clark, R. J. H.; Hester, R. E., Eds. Heyden & Son: London, 1982; pp 282-360.
- S4. Long, D. A., *The Raman Effect: A Unified Treatment of the Theory of Raman Scattering by Molecules*. Wiley: West Sussex, U.K., 2002.
- S5. Cotton, F. A., *Chemical Applications of Group Theory*. 3rd ed.; Wiley: 1990.
- S6. Mitchell, P. C. H.; Parker, S. F.; Ramirez-Cuesta, A. J.; Tomkinson, J., *Vibrational Spectroscopy with Neutrons: With Applications in Chemistry, Biology, Materials Science and Catalysis*. World Scientific Publishing Company: 2005; Vol. 3.